Hindawi
Journal of Nanomaterials
Volume 2021, Article ID 4945670, 15 pages
https://doi.org/10.1155/2021/4945670

Research Article

Nanolayered Double Hydroxide Inhibits the Pathogenicity of *Vibrio parahaemolyticus*

Cang Wang,[1,2] **Xiaoyi Ma**,[1,2] **Jie Hu**,[1,2] **Xiaopeng Tian**,[1,2] **Hao Zhang**,[1,2] **Dongxue Dong**,[1,2] **Zaixi Fang**,[1,2] **Mingsheng Lyu**,[1,2] **Shujun Wang**,[1,2] **and Jing Lu**[1,2]

[1]*Jiangsu Key Laboratory of Marine Bioresources and Environment/Jiangsu Key Laboratory of Marine Biotechnology, Jiangsu Ocean University, Lianyungang 222005, China*
[2]*Co-Innovation Center of Jiangsu Marine Bio-Industry Technology, Jiangsu Ocean University, Lianyungang 222005, China*

Correspondence should be addressed to Shujun Wang; sjwang@jou.edu.cn and Jing Lu; jinglu@jou.edu.cn

Received 23 July 2021; Revised 22 September 2021; Accepted 11 October 2021; Published 16 November 2021

Academic Editor: Haisheng Qian

Nanolayered double hydroxide (LDH) is a type of anion layered inorganic compound whose bacteriostatic properties have recently garnered much attention. *Vibrio parahaemolyticus* is a marine pathogen that can lead to aquaculture diseases and substantial economic losses. Therefore, our study assessed the mechanisms by which Mg/Al-LDH prevents *V. parahaemolyticus* infection. Our results demonstrated that Mg/Al-LDH not only inhibited *V. parahaemolyticus* growth but also biofilm formation. Moreover, coupling Mg/Al-LDH with hydrogen peroxide and UV irradiation further inhibited the growth and biofilm formation of *V. parahaemolyticus*. Additionally, Mg/Al-LDH was found to adversely affect DNA and the gelling ability of chitosan. Furthermore, exposing *V. parahaemolyticus* to Mg/Al-LDH led to a 54.73% and 4.3% inhibition in the expression of the toxic genes *tlh* and *trh*, respectively. Mg/Al-LDH also improved the symptoms of *V. parahaemolyticus* infection in *Penaeus vannamei*, making this a promising candidate to prevent pathogenic bacteria infection in aquaculture.

1. Introduction

Nanolayered double hydroxide (LDH), also known as anionic clay [1], is a type of anionic layered compound consisting of a positively charged metal hydroxide outlayer and a negative anion interlayer [2]. The molecular formula of LDH is $[M^{II}_{1-x}M^{III}_{x}(OH)_2]^{x+}(A^{n-})_{X/n}{\cdot}yH_2O$ ($x = 0.2 - 0.33$, $y = 0.5 - 1$), where M^{III} represents trivalent metal ions, M^{II} represents divalent metal ions, A^{n-} represents n-valent anions, and LDH represents the different structures that can be synthesized by changing the value of x [3, 4]. LDH can be cost-effectively prepared in the laboratory with good biocompatibility, adjustable layer charge density and particle size, low storage requirements, and low toxicity [1, 5]. LDH with various unique properties can be synthesized through different combinations of divalent metal ions and trivalent metal ions, as well as changes in proportion [1, 6]. LDH has many unique characteristics, including the adjustability of laminate element composition, exchangeability of the negative anion interlayer, thermal stability, pH sensitivity, and memory, all of which make this material uniquely well suited for a variety of applications in several fields such as biomedicine [7–9], adsorption [10–12], catalysis [13–15], and environmental remediation [16–18].

Particularly, the antibacterial properties of LDH have garnered much attention in recent years. Ding et al. [19] assessed LDH toxicity in *Chlorophyta* and found that this compound was highly toxic to *Streptococcus*, with an EC_{50} of 10 mg/L after 72 h of LDH exposure. Further, *Streptococcus* growth was completely inhibited when the LDH concentration reached 50 mg/L. An LDH prepared by Moaty et al. exhibited long-lasting antibacterial activity against Gram-negative bacteria (*Proteus vulgaris*, *Klebsiella pneumoniae*, *Escherichia coli*, and *Pseudomonas aeruginosa*) and Gram-positive bacteria (*Staphylococcus epidermidis*, *Staphylococcus aureus*, *Aspergillus*, *Streptococcus pyogenes*, and *Salmonella*)

[20]. Many studies have also confirmed that LDH has a good bacteriostatic effect when combined with other compounds or materials [21–25].

V. parahaemolyticus was first discovered by Tsunesaburo Fujino of Osaka University after a seafood poisoning outbreak in Japan in 1950 [26]. *V. parahaemolyticus* is a Gram-negative halophilic bacterium that is commonly found in estuaries and marine environments and various types of seafood [27], which can cause aquaculture diseases and considerable economic losses to the aquaculture industry. Moreover, people who consume raw or undercooked seafood are at high risk of becoming infected with *V. parahaemolyticus*. The symptoms of *V. parahaemolyticus* infection include diarrhea that lasts for 2 to 10 days, abdominal cramps, nausea, vomiting, and headaches [28]. Wound infection with *V. parahaemolyticus* can also lead to septicemia, which can be fatal [29–31]. Marine animals such as bony fish and grouper, mud crabs, and shrimp infected with *V. parahaemolyticus* often exhibit marked histopathological changes and increased mortality, thus resulting in huge economic losses to the aquaculture industry [32–34].

Several studies have evaluated the virulence factors and pathogenesis of *V. parahaemolyticus*. One such study found that the pathogenicity of *V. parahaemolyticus* was closely related to many virulence factors, including hemolysin, type III secretion system, type VI secretion system, adhesion factor, and iron uptake system [28, 35]. It has also been reported that *V. parahaemolyticus* produces three kinds of hemolysin: thermally stable direct hemolysin (*tdh*), tdh-associated hemolysin (*trh*), and heat-intolerant hemolysin (*tlh*), which are encoded by the *tdh*, *trh*, and *tlh* genes, respectively [36, 37]. Additionally, *V. parahaemolyticus* often forms biofilms and becomes embedded in its own extracellular polymeric matrix, making this pathogen uniquely resistant to cleaning and disinfection processes [38–40]. Therefore, biofilms protect microbial communities and facilitate quorum sensing.

Our study investigated the effects of exposed Mg/Al-LDH on *V. parahaemolyticus* when the Mg/Al-LDH and *V. parahaemolyticus* were exposed together. Furthermore, the mechanisms of effects were explored. The purpose is to reduce the chance of humans and aquaculture being infected with *V. parahaemolyticus*. Our findings indicated that Mg/Al-LDH prevented *V. parahaemolyticus* in *Penaeus vannamei*, thus highlighting the promising potential of Mg/Al-LDH as an antibacterial agent to increase aquaculture yields.

2. Materials and Methods

2.1. Materials and Strains. A *V. parahaemolyticus* strain was purchased from the China Industrial Microbial Culture Collection and Management Center (CICC 10552, ATCC17802, ATCC33846). Mg/Al-LDH was synthesized in the laboratory. TSB medium: tryptone 15 g, soybean peptone 5 g, NaCl 30 g, deionized water 1 L, pH 7.0~7.4; autoclaved at 121°C and 0.15 MPa for 20 min. 2216E medium: 1 g yeast powder, 5 g fish meal peptone, pH 7.4, seawater 1 L. Nutrient broth medium (3% NaCl): peptone 10 g beef extract 3 g, NaCl 30 g, pH 7.0. All reagents were of analytical grade.

Table 1: Primer sequences.

Primer	Sequence (5′-3′)
Tdh-F	GCT GCA TTC AAA ACA TCT GC TT
Tdh-R	CTC GAA CAA ACA ATA TCT CAT CA
Trh-F	GAG GAC TAT TGG ACA AAC CGA AA
Trh-R	TGT CAT ATA GGC GCT TAA CCA CTT
Tlh-F	CCA ACC TTA TCA CCA GAA
Tlh-R	ATA CCA ACA GCG AAC ATA
PvsA-F	CTC CTT CAT CCA ACA CGA T
PvsA-R	GGG CGA GAT AAT CCT TGT
PvuA-F	CAA ACT CAC TCA GAC TC
PvuA-R	CGA ACC GAT TCA ACA C

2.2. Effect of Mg/Al-LDH on V. parahaemolyticus Growth. V. parahaemolyticus was inoculated into TSB broth containing different Mg/Al-LDH concentrations (0-100 mg/L). The strain was incubated at 30°C and 180 r/min for 24 h, and the optical density at 600 nm was detected in a 96-well plate using a microplate reader (Infinite M1000 Pro, Tecan, Switzerland).

2.3. Effect of Mg/Al-LDH When Coupled with UV Irradiation or Hydrogen Peroxide. The activated *V. parahaemolyticus* was inoculated into media containing Mg/Al-LDH (100 mg/L) and then irradiated with ultraviolet light for 0-300 s. The strain was also grown without Mg/Al-LDH as a control treatment. Similarly, different concentrations of hydrogen peroxide (0-500 mM) were added to the growth media containing Mg/Al-LDH (100 mg/L), after which OD_{600} of the broth was measured.

2.4. Effect of Mg/Al-LDH on V. parahaemolyticus Biofilm Formation. V. parahaemolyticus biofilm formation was assessed as described by Yin et al. [40] with slight modifications. Specifically, this study explored the effect of Mg/Al-LDH on the biofilm formation of *V. parahaemolyticus*. The activated *V. parahaemolyticus* (50 μL), fresh medium, and Mg/Al-LDH were mixed in microplates to a 250 μL total volume. The final concentrations of Mg/Al-LDH were 0-100 mg/L. Then, the microplates were incubated at 30°C for 24 h. Afterward, the medium was removed and the wells were washed three times with 250 μL of phosphate-buffered saline (PBS). The microplates were then dried in a 60°C oven for 1 h. The biofilms were stained with 250 μL of 0.1% crystal violet solution at room temperature for 15 min. After gently washing the samples with PBS to remove excess crystal violet, the stained biofilm was dried again. Afterward, 250 μL of glacial acetic acid (30%) was added to dissolve the crystal violet stain and the optical density was measured at 590 nm.

Next, *V. parahaemolyticus* (50 μL), fresh medium, Mg/Al-LDH (100 mg/L), and hydrogen peroxide were mixed in microplates to a 250 μL total volume. The final hydrogen peroxide concentration ranged between 0 and 500 mM. A blank control was prepared without Mg/Al-LDH. Biofilm formation was detected after incubation.

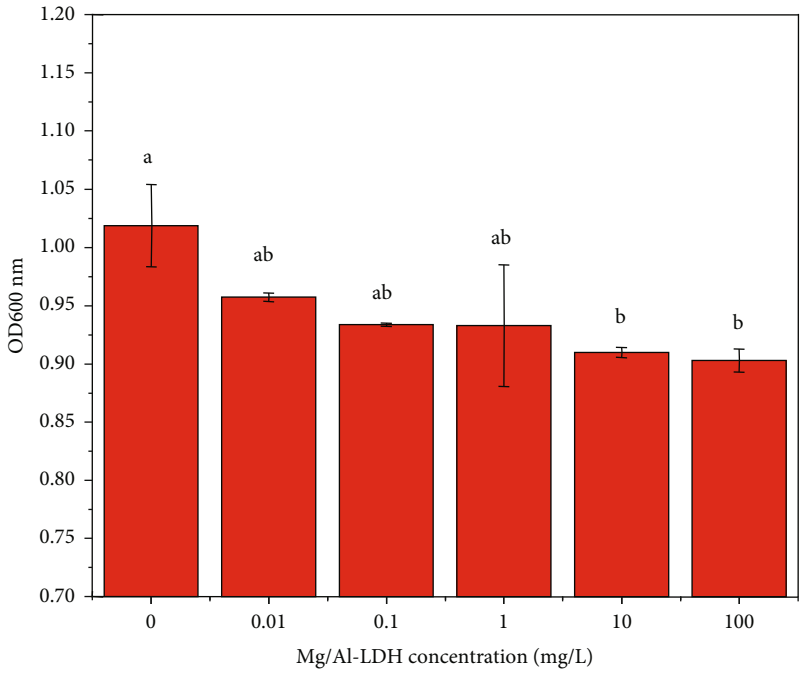

(a)

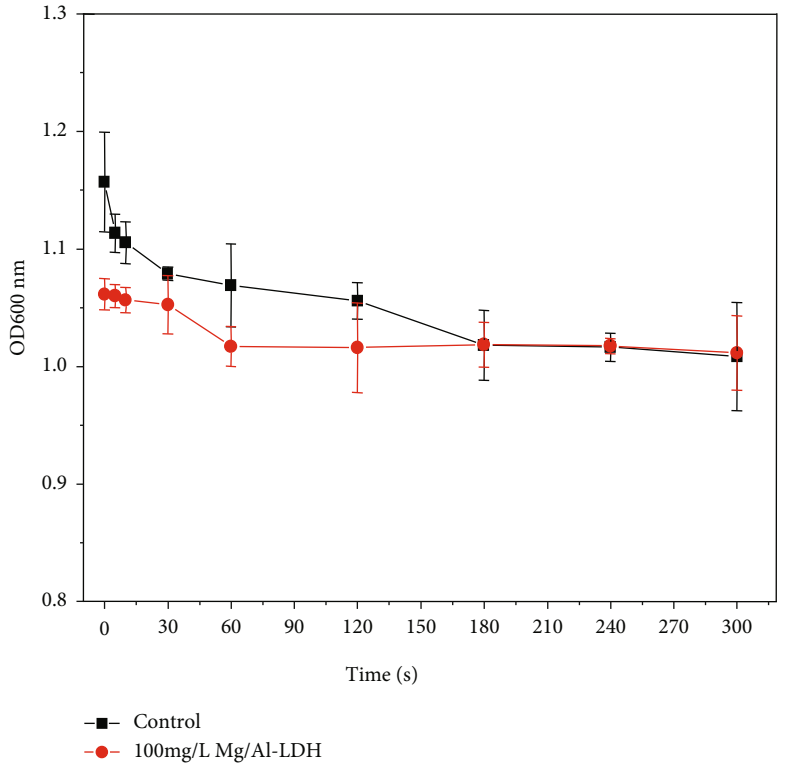

(b)

Figure 1: Continued.

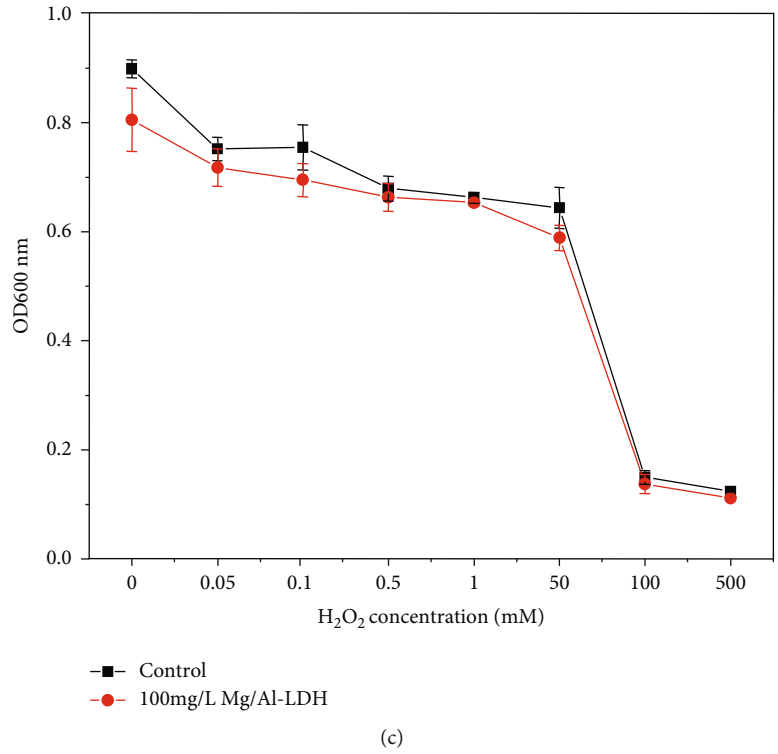

(c)

Figure 1: Effect of (a) Mg/Al-LDH concentration, (b) UV irradiation, and (c) hydrogen peroxide concentration on *V. parahaemolyticus* growth.

Finally, *V. parahaemolyticus* (50 μL), fresh medium, Mg/Al-LDH (100 mg/L), and hydrogen peroxide (50 mM) were mixed in microplates to a 250 μL total volume and then irradiated with ultraviolet light for 0-300 s. A blank control was prepared without Mg/Al-LDH. Biofilm formation was detected after incubation.

2.5. Effects of Mg/Al-LDH on Polysaccharides. Chitosan and 2.5% glutaraldehyde form a gel after being placed in a water bath at 70°C for 1 h. We then added 200 μL of 0.5% chitosan solution, 20 μL of 2.5% glutaraldehyde, and Mg/Al-LDH (100 mg/L) to glass bottles to a final 250 μL volume, after which they were treated with hydrogen peroxide (50 mM) and UV irradiation (2 min). The samples were taken out of the water bath (70°C) after 1 h. Upon gel formation, the weight of the gel was measured.

2.6. Effects of Mg/Al-LDH on Proteins. Bovine serum protein (BSA) is a typical functional protein. A 250 μL system was prepared by mixing Mg/Al-LDH (100 mg/L), bovine serum protein, followed by hydrogen peroxide (50 mM) or UV irradiation (2 min). SDS-PAGE gel electrophoresis and quantitative analysis were then performed after incubation for 2 h in a 37°C water bath.

2.7. Effects of Mg/Al-LDH on DNA Integrity. Salmon DNA was added to a 50 μL system with Mg/Al-LDH (100 mg/L), hydrogen peroxide (50 mM), or UV irradiation (2 min) and then incubated in a 37°C water bath for 2 h. Afterward, 1% agar electrophoresis was conducted for verification and quantitative analysis was performed using a microanalyzer.

2.8. Effect of Mg/Al-LDH on V. parahaemolyticus Toxicity Genes. SYBR staining was used to quantify the relative expression of toxicity genes using an internal reference. *V. parahaemolyticus* ATCC33846 (2216E medium, 30°C) and *V. parahaemolyticus* ATCC17802 (3% NaCl nutrient gravy medium, 37°C) were incubated at 180 r/min for 12 h. The *V. parahaemolyticus* strains exposed to Mg/Al-LDH (100 mg/L) were then continually cultured. DNA was extracted separately for later use. The expression of the toxic genes *trh*, *tdh*, and *tlh* of *V. parahaemolyticus* in response to Mg/Al-LDH exposure was detected via fluorescence quantitative PCR and compared to that of unexposed bacteria. The primer sequences are shown in Table 1. The reactions were conducted in 20 μL volumes (2x ChamQ SYBR qPCR Master Mix (10 μL), forward primer (10 μM; 0.8 μL), reverse primer (10 μM; 0.8 μL), 50x ROX Reference Dye (0.4 μL), DNA (4 μL), ddH_2O (4 μL)).

2.9. P. vannamei Infection Experiments. Healthy white shrimp (*P. vannamei*; 6 cm long) were purchased from the Lianyungang Wholesale Market. Twelve *P. vannamei* were placed in each water tank outfitted with a circulating filter device to maintain water quality. The water temperature and salinity of the water tank were controlled to 25°Cand 20‰, respectively. Once the shrimp were adapted to the growth environment, 20 mL of *V. parahaemolyticus* (ATCC17802; 1.21×108 CFU/mL) was added to

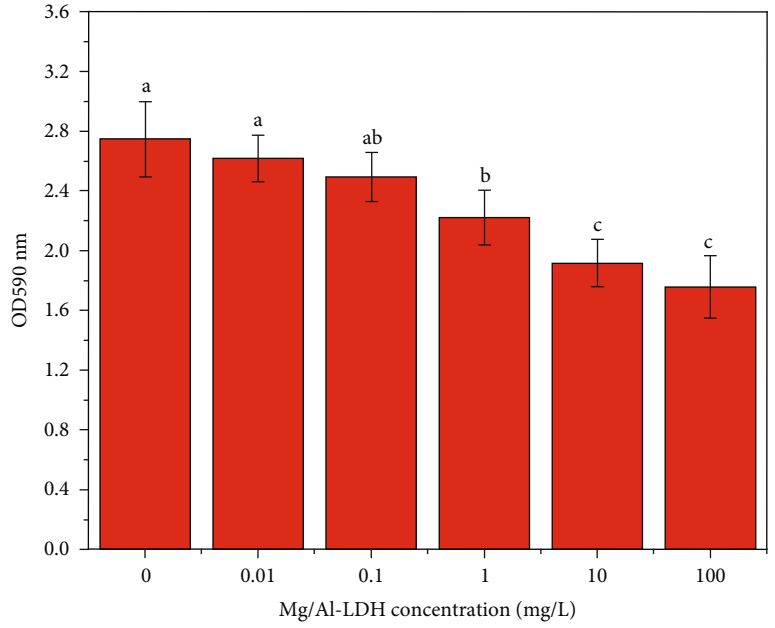

(a)

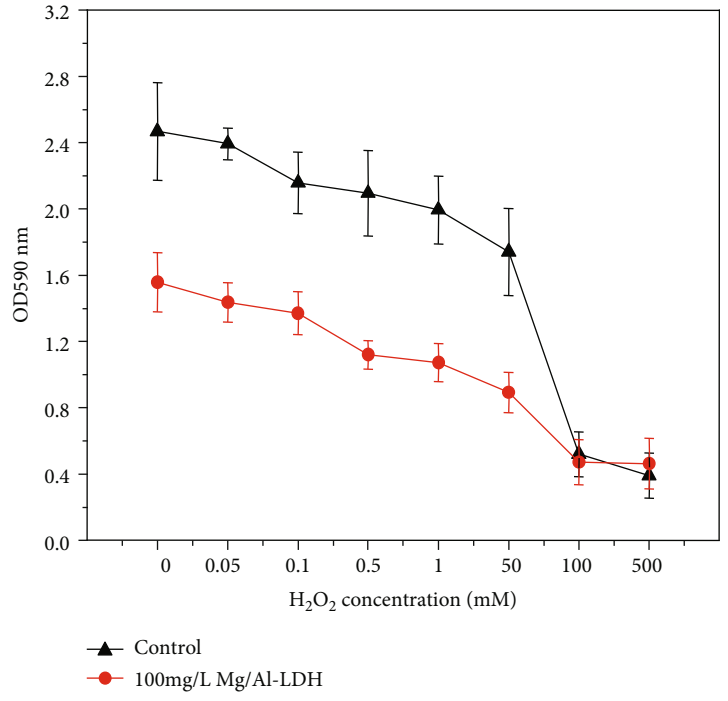

(b)

Figure 2: Continued.

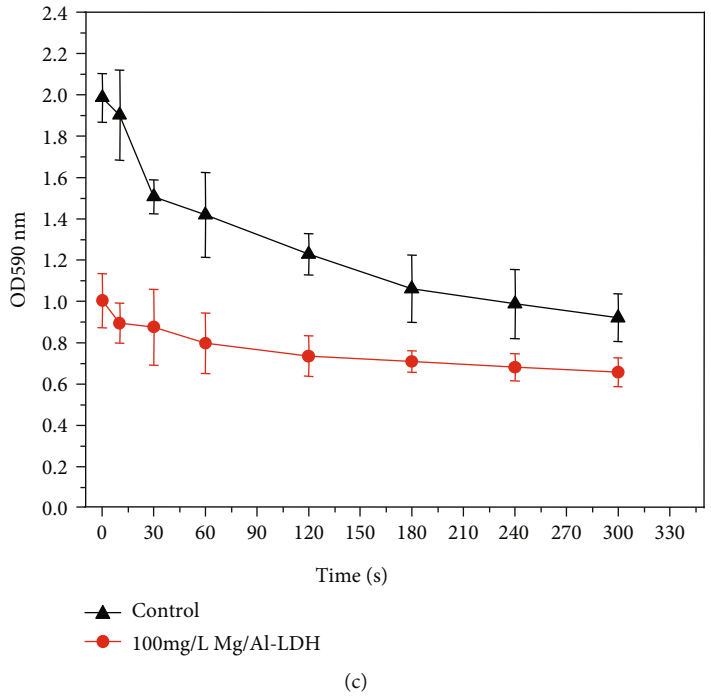

(c)

Figure 2: Effects of (a) Mg/Al-LDH concentration, (b) hydrogen peroxide concentration, and (c) UV irradiation time on *V. parahaemolyticus* biofilm formation.

experimental groups 1 and 2. Afterward, 100 mg/mL of Mg/Al-LDH was added to experimental group 2. The control was neither infected with *V. parahaemolyticus* nor treated with Mg/Al-LDH. The shrimp were fed once every 24 h; infection progression and mortality were monitored every day.

2.10. Statistical Analysis. All experiments were conducted in triplicate, from which means and standard deviations were calculated. Significance was conducted using the S-N-K(S) test in SPSS.

3. Results and Discussion

3.1. Results

3.1.1. Effect of Mg/Al-LDH on V. parahaemolyticus Growth. Mg/Al-LDH significantly inhibited *V. parahaemolyticus* growth at a 100 mg/L concentration (Figure 1(a)), with OD values reaching only 90% compared to the control. The growth of *V. parahaemolyticus* treated with Mg/Al-LDH was more severely inhibited within a short time of UV irradiation (Figure 1(b)). However, once the irradiation time reached 2 min, the growth inhibition of *V. parahaemolyticus* was largely unaffected by Mg/Al-LDH. Combining hydrogen peroxide with Mg/Al-LDH had a stronger inhibitory effect on the growth of the strain. Particularly, hydrogen peroxide concentrations ranging from 0 to 50 mM effectively inhibited the growth of *V. parahaemolyticus* when coupled with Mg/Al-LDH (100 mg/L) (Figure 1(c)). However, when the concentration of hydrogen peroxide reached 100 mM, the turbidity of the bacterial liquid was lower than 0.2. At this point, bacterial growth was mainly inhibited by hydrogen peroxide. Therefore, Mg/Al-LDH (100 mg/L) inhibited *V. parahaemolyticus* growth most efficiently when combined with low concentrations of hydrogen peroxide.

3.1.2. Effect of Mg/Al-LDH on V. parahaemolyticus Biofilm Formation. We next assessed the effect of Mg/Al-LDH on the formation of *V. parahaemolyticus* biofilm. With increasing Mg/Al-LDH concentrations, *V. parahaemolyticus* biofilm formation was gradually inhibited (Figure 2(a)). The results showed that OD_{590} decreased from 2.75 to 1.76 and the inhibition rate reached 36%.

V. parahaemolyticus biofilms were severely damaged during the formation process (Figure 2(b)). As the concentration of hydrogen peroxide increased, the biofilm of the experimental group was more severely damaged. However, when the concentration of hydrogen peroxide reached 100 mM, the growth of *V. parahaemolyticus* was severely inhibited and biofilm formation was reduced. At this point, Mg/Al-LDH had little effect on *V. parahaemolyticus* biofilm formation. However, when the concentration of hydrogen peroxide was 50 mM, the growth of *V. parahaemolyticus* was not severely inhibited. The results showed that OD_{590} of the control group was 1.74 and OD_{590} of the experimental group treated with Mg/Al-LDH was 0.89.

The effects of UV irradiation coupled with hydrogen peroxide and Mg/Al-LDH on *V. parahaemolyticus* biofilm formation in microplates were also assessed. *V. parahaemolyticus* biofilm formation was more severely inhibited when all three factors were combined. Our results demonstrated that OD_{590} of the control group decreased from 1.99 to 0.92, indicating that the biofilm formation could be inhibited

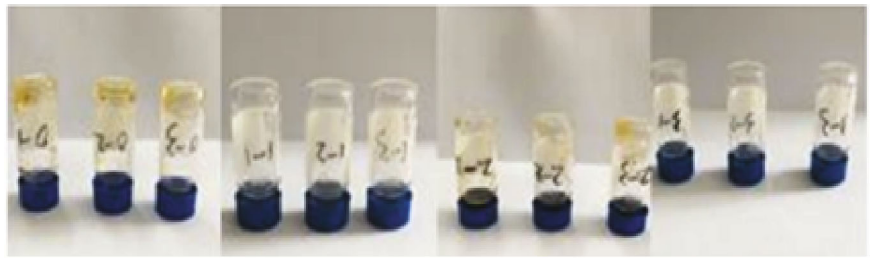

1 2 3 4

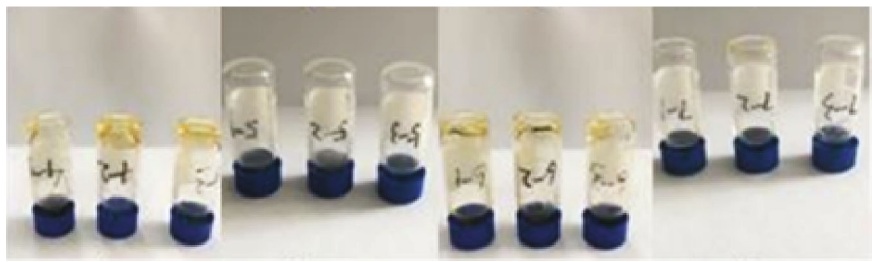

5 6 7 8

(a)

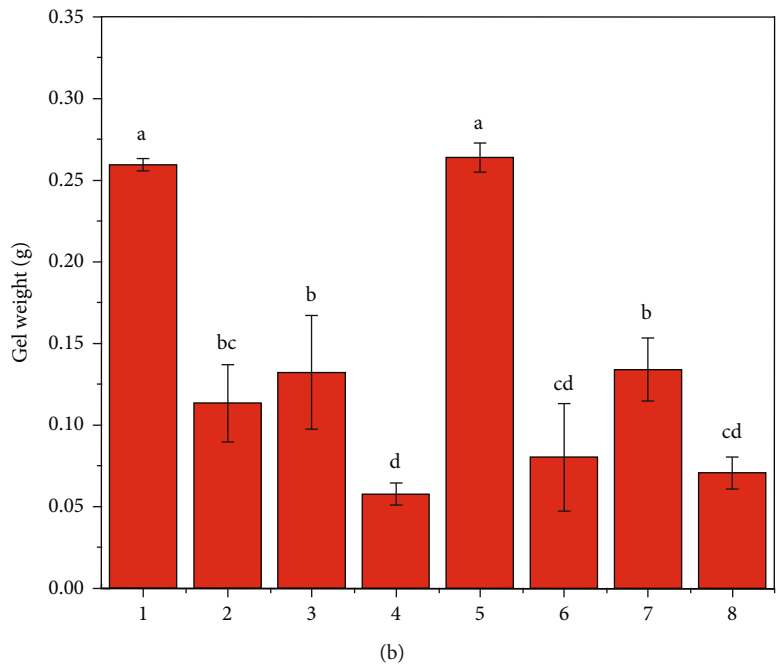

(b)

Figure 3: Continued.

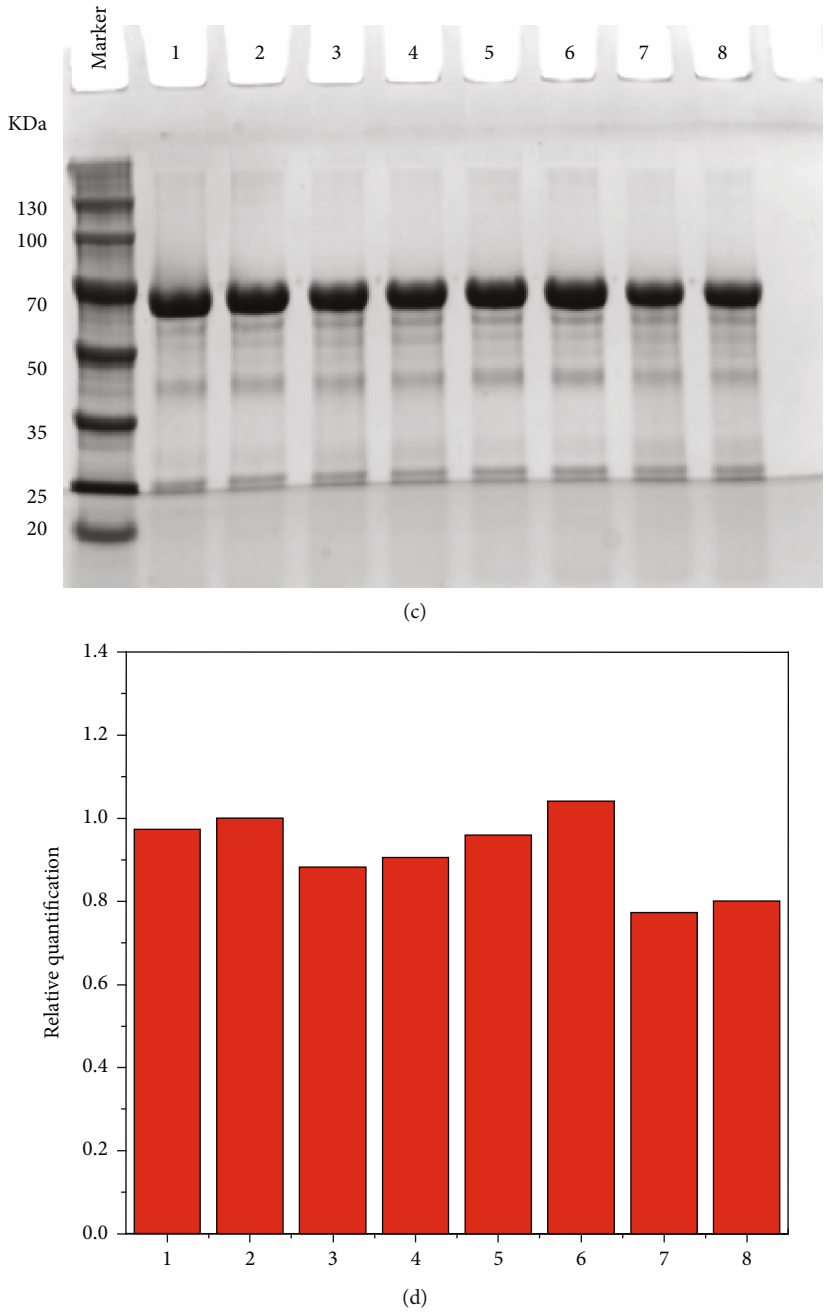

Figure 3: (a) Affection on polysaccharide gel and (b) weight analysis of the polysaccharide gels. The numbers in (a) and (b) indicate (1) chitosan, (2) chitosan+LDH, (3) chitosan+H_2O_2, (4) chitosan+H_2O_2+LDH, (5) chitosan+UV, (6) chitosan+LDH+UV, (7) chitosan+H_2O_2 +UV, and (8) chitosan+LDH+H_2O_2+UV. (c) SDS-PAGE gel electrophoresis of bovine serum albumin after 2 hours in a water bath. (d) Quantitative analysis of the relative quality of the SDS-PAGE BSA electrophoresis. The numbers in (c) and (d) represent (1) BSA, (2) BSA+LDH, (3) BSA+H_2O_2, (4) BSA+H_2O_2+LDH, (5) BSA+UV, (6) BSA+LDH+UV, (7) BSA+H_2O_2+UV, and (8) BSA+LDH+H_2O_2+UV.

by UV irradiation and the inhibition increased with increasing irradiation time (Figure 2(c)). In the experimental group, OD_{590} decreased from 1.01 to 0.66.

3.1.3. Effects of Mg/Al-LDH on Polysaccharides. Chitosan and glutaraldehyde undergo a gelling reaction when heated to 70°C. However, upon adding Mg/Al-LDH (100 mg/L), the gelling reaction is greatly reduced. This indicated that Mg/Al-LDH can inhibit the gelation ability of polysaccharides. Moreover, polysaccharides were further weakened when treated with Mg/Al-LDH, hydrogen peroxide, and UV light (Figure 3(b)).

3.1.4. Effect of Mg/Al-LDH on Protein. Based on the comparisons between 1 and 2, 3 and 4, 5 and 6, and 7 and 8 in Figure 3(d), the protein residue in the experimental group with Mg/Al-LDH was slightly higher than that without Mg/Al-LDH. However, as illustrated by the comparison between 2 and 8, the most significant protein degradation

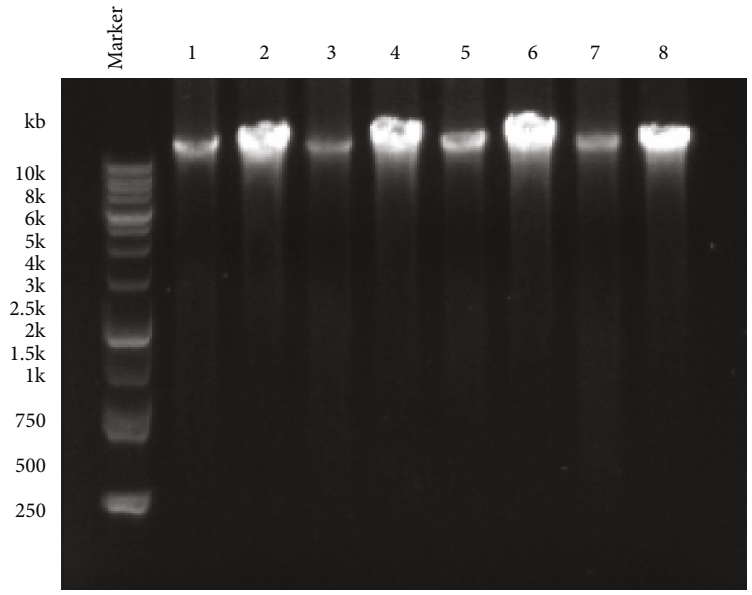

(a)

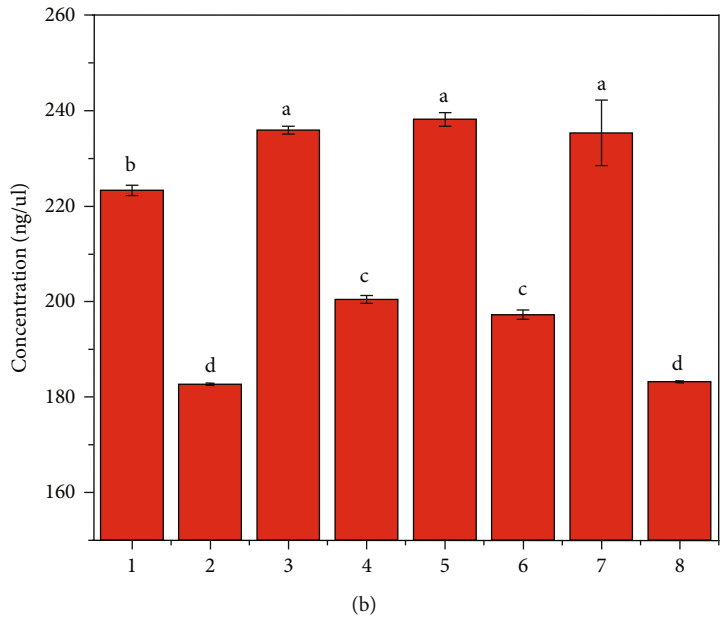

(b)

Figure 4: Continued.

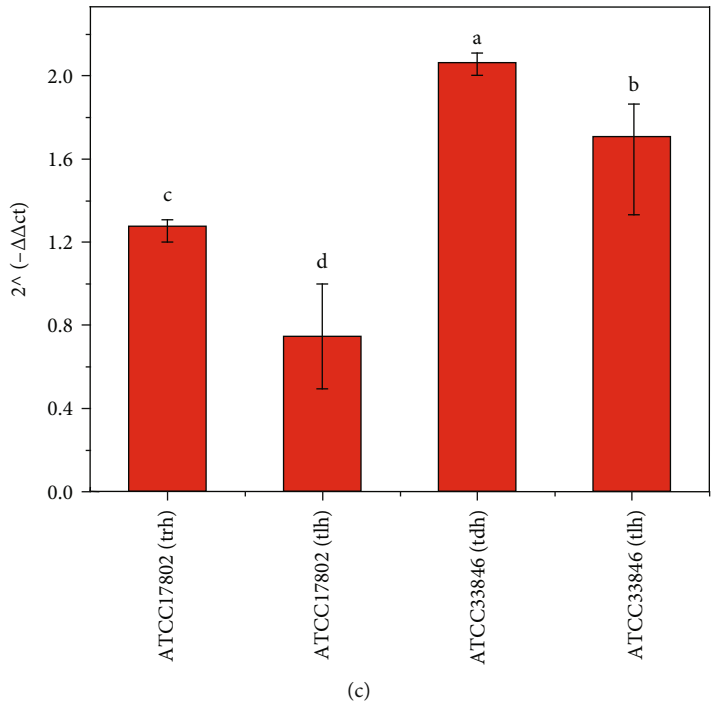

Figure 4: (a) Agarose gel electrophoresis after DNA water bath for 2 hours. (b) Quantitative analysis of DNA with a microanalyzer. The numbers in (a) and (b) represent (1) DNA, (2) DNA+LDH, (3) DNA+H_2O_2, (4) DNA+H_2O_2+LDH, (5) DNA+UV, (6) DNA+LDH+UV, (7) DNA+H_2O_2+UV, and (8) DNA+LDH+H_2O_2+UV. (c) Effects of Mg/Al-LDH on the expression of *V. parahaemolyticus* virulence genes.

effect was obtained when Mg/Al-LDH, hydrogen peroxide, and ultraviolet light were combined.

3.1.5. Effect of Mg/Al-LDH on DNA. Our study also explored whether DNA is degraded under Mg/Al-LDH, hydrogen peroxide, and ultraviolet conditions. To achieve this, DNA, Mg/Al-LDH, and hydrogen peroxide were mixed, irradiated with UV rays, and incubated in a 37°C water bath for 2 h. After subsequent quantitative analysis using a microanalyzer, the values of 1, 3, 5, and 7 were all higher than those of 2, 4, 6, and 8 (Figure 4(b)). This indicated that Mg/Al-LDH addition caused DNA degradation.

3.1.6. Effect of Mg/Al-LDH on the Expression of Toxicity-Associated Genes in V. parahaemolyticus. The extracted DNA was quantitatively analyzed via fluorescence quantitative PCR. As shown in Figure 4(c), Mg/Al-LDH exerted 4.3% and 54.73% inhibition rates for the *trh* and *tlh* genes of strain ATCC17802. In contrast, Mg/Al-LDH promoted the expressions of the *tdh* and *tlh* genes by 60.21% and 35.19% in the ATCC33846 strain.

3.1.7. Infection Experiment. The shrimps (*P. vannamei*) were placed in each water tank outfitted with a circulating filter (Figure 5(a)). After breeding for a period of time under different conditions, as illustrated in Figures 5(b) and 5(c), the symptoms of *P. vannamei* upon *V. parahaemolyticus* infection in experimental group 1 were more severe than those in experimental group 2. The shrimp in experimental group 2 did not appear sluggish but presented hepatopancreas ulcers and hyperemia. Ulcers were not detected in the parotid glands, tail fans, appendages, and swimming appendages. Additionally, as illustrated in Figure 5(d), shrimp mortality in experimental group 2 was much lower than that in experimental group 1 after 3-11 days of infection.

3.2. Discussion. Mg/Al-LDH significantly inhibited *V. parahaemolyticus* growth that was consistent with the excellent antibacterial properties of Zn/Fe-LDH reported by Moaty et al. on several common bacteria such as *Pseudomonas aeruginosa* and *Staphylococcus aureus* [20]. Previous studies have shown that LDHs had a strong inhibitory effect on the growth of some pathogenic bacteria and might therefore be used to treat and prevent bacterial infection. Ultraviolet (UV) light, an important component of Earth's natural lighting, kills microorganisms by changing and damaging the structure of their DNA [41]. Particularly, UVC can effectively kill bacteria, viruses, protists, and other microorganisms [42] and is therefore often used as a disinfectant. Within a short time of UV irradiation, the growth of *V. parahaemolyticus* treated with Mg/Al-LDH was more severely inhibited. This may have been because short-term UVC irradiation destroyed the DNA of *V. parahaemolyticus*, thereby inhibiting its growth. The decomposition of hydrogen peroxide can produce free radicals, which can inactivate microorganisms by interfering with cell membranes, DNA, and proteins [43, 44]. Therefore, combining hydrogen peroxide with Mg/Al-LDH had a stronger inhibitory effect on the growth of the strain.

Biofilms are composed of a variety of biological macromolecules such as proteins, polysaccharides, DNA, RNA,

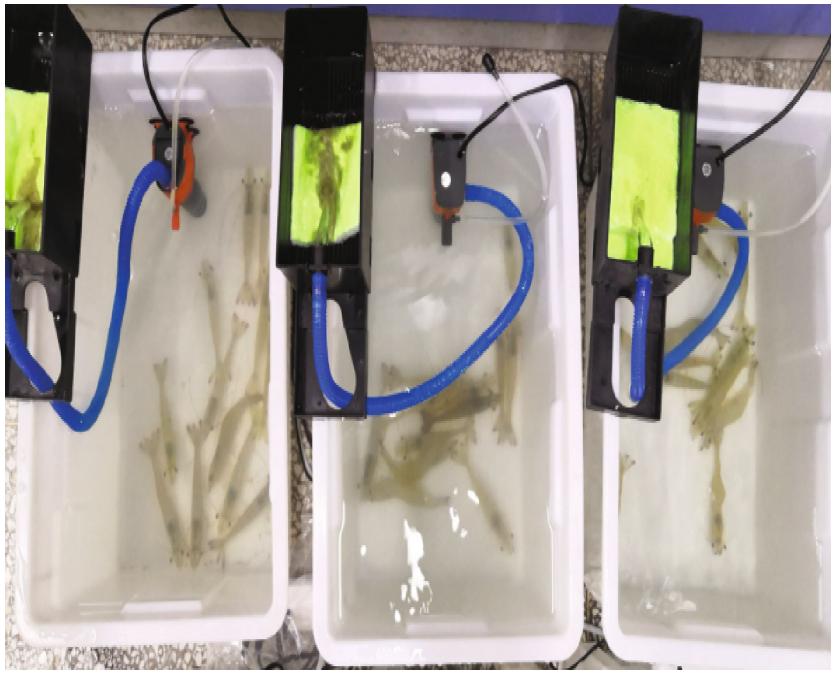

(a)

Symptoms of infection	Control	Experimental group 1	Experimental group 2
Hepatopancreas fester and hyperemia	–	++	–
Parotid gland fester and hyperemia	–	++	+
Tail fan fester and hyperemia	–	++	+
Appendages, swimming feet fester and hyperemia	–	++	+
Whole body hyperemia	–	+	–
Sluggish action	–	++	–
Deaths	0	12	7

(b)

Figure 5: Continued.

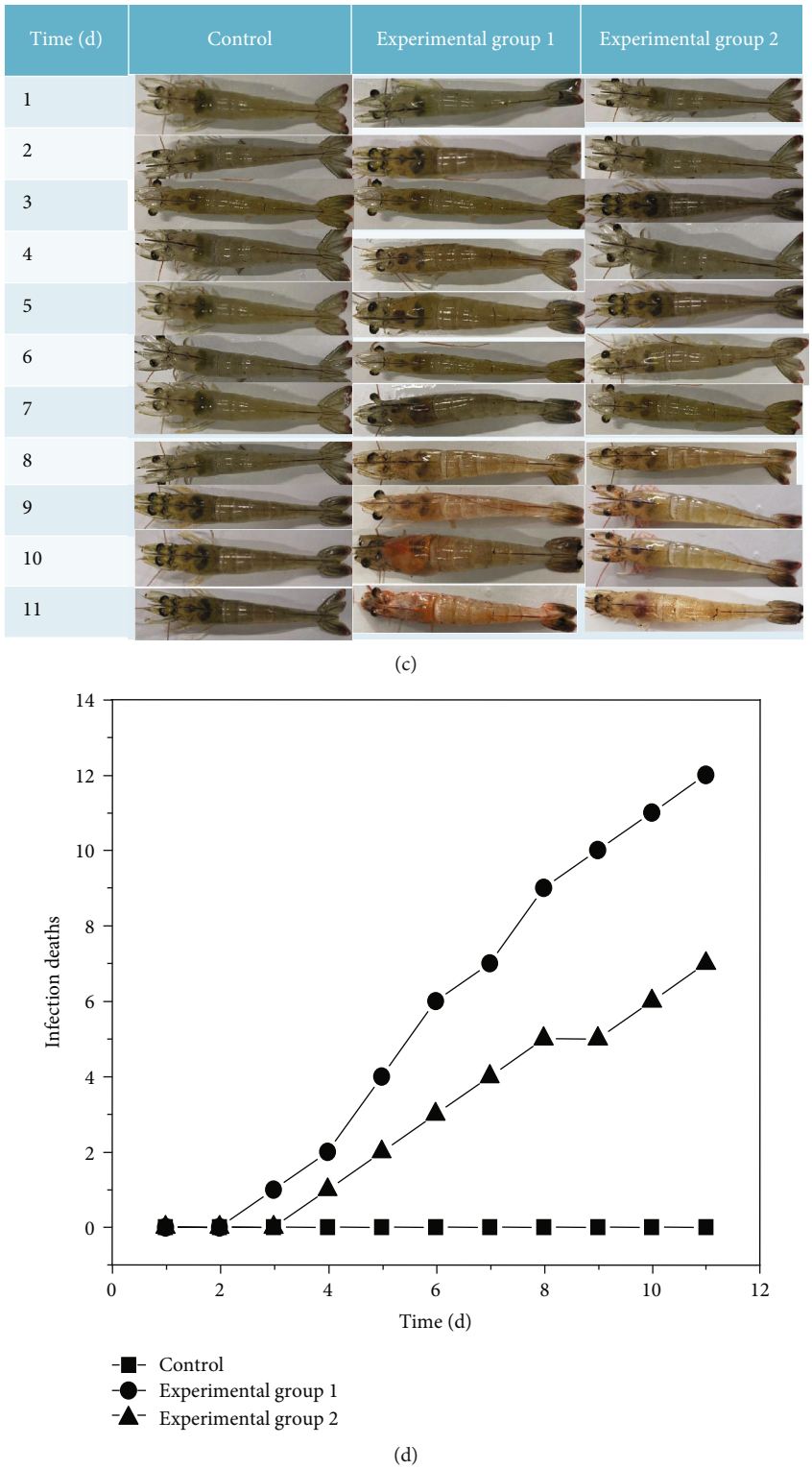

Figure 5: (a) Experimental environment. (b) Evaluation of infection symptoms. (c) Impact of different treatments on *Penaeus vannamei*. (d) Mortality rates upon infection. Experimental group 1: *V. parahaemolyticus*. Experimental group 2: *V. parahaemolyticus* and Mg/Al-LDH.

peptidoglycans, lipids, and phospholipids. These complex matrices render bacteria highly resistant to antibiotics, as well as cleaning and disinfection processes [40]. Adding Mg/Al-LDH could effectively inhibit the formation of biofilms that might be because Mg/Al-LDH destroys major macromolecules such as polysaccharides and DNA during biofilm formation. And hydrogen peroxide, Mg/Al-LDH, and UV irradiation could inhibit the formation of *V.*

parahaemolyticus biofilm more effectively, in which hydrogen peroxide and ultraviolet radiation can destroy the biofilm to varying degrees.

Chitosan is a natural polysaccharide derived from chitin. It is the second most ubiquitous naturally occurring polysaccharide after cellulose. Chitosan is obtained when chitin is deacetylated to approximately 50% of free amines. As a biopolymer, chitosan has attracted much attention due to its biomedical applications [45]. In our study, Mg/Al-LDH can inhibit the gelation ability of polysaccharides. This might be because Mg/Al-LDH was adsorbed on the polysaccharide, thus affecting its gelling ability.

Bovine serum albumin (BSA), a typical functional protein molecule, is cost-efficient, safe, degradable, rich in chemical groups, and relatively stable, all of which make this protein uniquely well suited for medical care and pharmaceutical applications [46]. Our research results showed that Mg/Al-LDH did not degrade bovine serum proteins. Therefore, we speculated that Mg/Al-LDH may not disrupt most proteins in cells. In many reports, LDH is used for drug delivery [47]. Mg/Al-LDH was likely adsorbed on the protein, thus preventing its degradation.

Deoxyribonucleic acid (DNA) is a kind of polynucleotide that carries essential genetic information and can be used to encode messenger RNA and proteins. DNA has been widely used in gene therapy, biosensing, and information storage. But Mg/Al-LDH could degrade salmon DNA. Therefore, Mg/Al-LDH may damage the DNA of *V. parahaemolyticus*, which provides an important basis for the further exploration of the molecular mechanisms of Mg/Al-LDH-mediated antibacterial effects. The results of subsequent toxic gene experiments were also consistent with these observations. It was confirmed that Mg/Al-LDH can inhibit the expression of virulence-associated genes in some *V. parahaemolyticus* strains. Therefore, our findings indicated that Mg/Al-LDH not only inhibits the growth of *V. parahaemolyticus* but also downregulates the expression of toxic genes.

Shrimp mortality in experimental group 2 was much lower than that in experimental group 1 after infection. These observations were consistent with our previous results, thus confirming that Mg/Al-LDH can inhibit the pathogenicity of *V. parahaemolyticus*. This was mainly due to the cytotoxicity of Mg/Al-LDH to *V. parahaemolyticus*, which disrupts its biofilm and affects the expression of toxic genes. Ahmed et al. [48] reported that the effect of nanoparticles (NPs) on bacteria mainly depends on certain mechanisms, including the interaction with cell barriers, penetration through diffusion and adsorption, inhibition of bacterial proteins and DNA synthesis, regulation of metabolic gene expression, and inhibition of biofilm formation.

4. Conclusions

LDH, a novel low-toxicity nanomaterial, plays an important role in various industries. In this study, this nanomaterial was used to prevent and control bacterial infection in Pacific white leg shrimp (i.e., a widely cultured aquaculture species).

The following are the key conclusions of this study:

(1) Mg/Al-LDH had a certain inhibitory effect on the growth of *V. parahaemolyticus*, which could be enhanced when coupled with hydrogen peroxide and UV irradiation

(2) Mg/Al-LDH also effectively inhibited *V. parahaemolyticus* biofilm formation. However, the addition of hydrogen peroxide and UV radiation did not significantly enhance the inhibitory effects of Mg/Al-LDH on *V. parahaemolyticus* biofilm formation

(3) Mg/Al-LDH inhibited the chitosan gelling reaction, and this effect was further enhanced by hydrogen peroxide addition. Moreover, Mg/Al-LDH had a weak protective effect on bovine serum protein. Mg/Al-LDH also caused considerable DNA damage

(4) Mg/Al-LDH inhibited the expression of the *trh* and *tlh* genes of strain ATCC17802 by 4.3% and 54.73%, respectively

(5) Our infection experiments indicated that the addition of Mg/Al-LDH could reduce *Penaeus vannamei* mortality caused by *V. parahaemolyticus* infection

These five conclusions confirm the important role of Mg/Al-LDH in the prevention and treatment of *V. parahaemolyticus*. Therefore, our study provides a robust basis for the development of novel strategies to protect human health and control bacterial diseases in the seafood industry.

Data Availability

The data used to support the findings of this study are included within the article.

Conflicts of Interest

All authors have declared that (i) no support, financial or otherwise, has been received from any organization that may have an interest in the submitted work and (ii) there are no other relationships or activities that could appear to have influenced the submitted work.

Authors' Contributions

Cang Wang and Xiaoyi Ma contributed equally to this work.

Acknowledgments

This study was supported by the National Key R&D Program of China (2018YFC0311106), the Priority Academic Program Development of Jiangsu Higher Education Institutions (PAPD), and the Research & Practice Innovation Program of Jiangsu (SJCX19-2297 and ZD201918).

References

[1] A. Chatterjee, P. Bharadiya, and D. Hansora, "Layered double hydroxide based bionanocomposites," *Applied Clay Science*, vol. 177, pp. 19–36, 2019.

[2] X. Bi, H. Zhang, and L. Dou, "Layered double hydroxide-based nanocarriers for drug delivery," *Pharmaceutics*, vol. 6, no. 2, pp. 298–332, 2014.

[3] G. Mishra, B. Dash, S. Pandey, and D. Sethi, "Ternary layered double hydroxides (LDH) based on Cu- substituted Zn![single bond](https://sdfestaticassets-eu-west-1.sciencedirectassets.-com/shared- assets/55/entities/sbnd.gif)Al for the design of efficient antibacterial ceramics," *Applied Clay Science*, vol. 165, pp. 214–222, 2018.

[4] D. Yan, J. Lu, L. Chen et al., "A strategy to the ordered assembly of functional small cations with layered double hydroxides for luminescent ultra-thin films," *Chemical Communications*, vol. 46, no. 32, pp. 5912–5914, 2010.

[5] D. G. Evans and X. Duan, "Preparation of layered double hydroxides and their applications as additives in polymers, as precursors to magnetic materials and in biology and medicine," *Chemical Communications*, vol. 37, no. 5, pp. 485–496, 2006.

[6] A. Khan, "Intercalation chemistry of layered double hydroxides: recent developments and applications," *ChemInform*, vol. 12, no. 11, pp. 3191–3198, 2002.

[7] V. Rives, M. del Arco, and C. Martín, "Intercalation of drugs in layered double hydroxides and their controlled release: a review," *Applied Clay Science*, vol. 88-89, pp. 239–269, 2014.

[8] S. Saha, S. Ray, R. Acharya, T. K. Chatterjee, and J. Chakraborty, "Magnesium, zinc and calcium aluminium layered double hydroxide-drug nanohybrids: a comprehensive study," *Applied Clay Science*, vol. 135, pp. 493–509, 2016.

[9] S. U. Muhammad, H. Mohd, F. Sharida, M. Mas, and A. S. Fathinul, "Gadolinium-doped gallic acid-zinc/aluminium-layered double hydroxide/gold theranostic nanoparticles for a bimodal magnetic resonance imaging and drug delivery system," *Nanomaterials*, vol. 7, no. 9, 2017.

[10] H. Yan, Q. Chen, J. Liu, Y. Feng, and K. Shih, "Phosphorus recovery through adsorption by layered double hydroxide nano- composites and transfer into a struvite-like fertilizer," *Water Research*, vol. 145, pp. 721–730, 2018.

[11] T. Hibino, "Deterioration of anion-adsorption abilities of layered double hydroxides synthesized in agarose gel," *Applied Clay Science*, vol. 186, p. 105435, 2020.

[12] M. Rosset, L. W. Sfreddo, O. W. Perez-Lopez, and L. A. Féris, "Effect of concentration in the equilibrium and kinetics of adsorption of acetylsalicylic acid on ZnAl layered double hydroxide," *Journal of Environmental Chemical Engineering*, vol. 8, no. 4, p. 103991, 2020.

[13] S. A. Hosseini, M. Davodian, and A. R. Abbasian, "Remediation of phenol and phenolic derivatives by catalytic wet peroxide oxidation over Co-Ni layered double nano hydroxides," *Journal of the Taiwan Institute of Chemical Engineers*, vol. 75, pp. 97–104, 2017.

[14] R. Dou, J. Ma, D. Huang et al., "Bisulfite assisted photocatalytic degradation of methylene blue by Ni-Fe-Mn oxide from MnO_4 intercalated LDH," *Applied Clay Science*, vol. 161, pp. 235–241, 2018.

[15] R. Gao, J. Zhu, and D. Yan, "Transition metal-based layered double hydroxides for photo(electro)chemical water splitting: a mini review," *Nanoscale*, vol. 13, no. 32, pp. 13593–13603, 2021.

[16] P. Gu, S. Zhang, X. Li et al., "Recent advances in layered double hydroxide-based nanomaterials for the removal of radionuclides from aqueous solution," *Environmental Pollution*, vol. 240, pp. 493–505, 2018.

[17] M. Darie, E. M. Seftel, M. Mertens, R. G. Ciocarlan, P. Cool, and G. Carja, "Harvesting solar light on a tandem of Pt or Pt-Ag nanoparticles on layered double hydroxides photocatalysts for p-nitrophenol degradation in water," *Applied Clay Science*, vol. 182, p. 105250, 2019.

[18] F. Wang and Z. Guo, "Insitu growth of ZIF-8 on Co![single bond](https://sdfestaticassets-eu- west-1.sciencedirectassets.-com/shared-assets/55/entities/sbnd.gif)Al layered double hydroxide/carbon fiber composites for highly efficient absorptive removal of hexavalent chromium from aqueous solutions," *Applied Clay Science*, vol. 175, pp. 115–123, 2019.

[19] T. Ding, K. Lin, J. Chen et al., "Causes and mechanisms on the toxicity of layered double hydroxide (LDH) to green algae _Scenedesmus quadricauda_," *The Science of the Total Environment*, vol. 635, pp. 1004–1011, 2018.

[20] S. A. A. Moaty, A. A. Farghali, and R. Khaled, "Preparation, characterization and antimicrobial applications of Zn-Fe LDH against MRSA," *Materials for Biogical applications*, vol. 68, pp. 184–193, 2016.

[21] M. Wang, Q. Hu, D. Liang et al., "Intercalation of Ga^{3+}-salicylidene-amino acid Schiff base complexes into layered double hydroxides: Synthesis, characterization, acid resistant property, in vitro release kinetics and antimicrobial activity," *Applied Clay Science*, vol. 83-84, pp. 182–190, 2013.

[22] S. Kim, J. Fahel, P. Durand, E. Andre, and C. CARTERET, "Ternary layered double hydroxides (LDHs) based on Co-, Cu-Substituted ZnAl for the Design of efficient photocatalysts," *European Journal of Inorganic Chemistry*, vol. 2017, no. 3, pp. 669–678, 2017.

[23] G. Mishra, B. Dash, and S. Pandey, "Layered double hydroxides: a brief review from fundamentals to application as evolving biomaterials," *Applied Clay Science*, vol. 153, pp. 172–186, 2017.

[24] M. Li, Y. Sultanbawa, Z. P. Xu et al., "High and long-term antibacterial activity against _Escherichia coli_ via synergy between the antibiotic penicillin G and its carrier ZnAl layered double hydroxide," *Colloids and Surfaces B: Biointerfaces*, vol. 174, pp. 435–442, 2019.

[25] G. Mishra, B. Dash, and S. Pandey, "Effect of molecular dimension on gallery height, release kinetics and antibacterial activity of Zn![single bond](https://sdfestaticassets-eu- west-1.sciencedirectassets.com/shared-assets/55/entities/sbnd.gif)Al layered double hydroxide (LDH) encapsulated with benzoate and its derivatives," *Applied Clay Science*, vol. 181, p. 105230, 2019.

[26] S. U. M. I. O. SHINODA, "Sixty years from the discovery of Vibrio parahaemolyticus and some recollections," *Biocontrol Science*, vol. 16, no. 4, pp. 129–137, 2011.

[27] Y. Jiang, Y. Chu, G. Xie et al., "Antimicrobial resistance, virulence and genetic relationship of _Vibrio parahaemolyticus_ in seafood from coasts of Bohai Sea and Yellow Sea, China," *International Journal of Food Microbiology*, vol. 290, pp. 116–124, 2019.

[28] L. Li, H. Meng, D. Gu, Y. Li, and M. Jia, "Molecular mechanisms of _Vibrio parahaemolyticus_ pathogenesis," *Microbiological Research*, vol. 222, pp. 43–51, 2019.

[29] T. Honda and T. Iida, "The pathogenicity of Vibrio parahaemolyticus and the role of the thermostable direct haemolysin and related haemolysins," *Reviews in Medical Microbiology*, vol. 4, no. 2, pp. 106–113, 1993.

[30] C. A. Broberg, T. J. Calder, and K. Orth, "_Vibrio parahaemolyticus_ cell biology and pathogenicity determinants," *Microbes and Infection*, vol. 13, no. 12-13, pp. 992–1001, 2011.

[31] C. Baker-Austin, J. D. Oliver, M. Alam et al., "_Vibrio_ spp. infections," *Nature Reviews Disease Primers*, vol. 4, no. 1, pp. 1–19, 2018.

[32] W. Peng, Y. Shi, G. F. Li et al., "_Tetraodon nigroviridis_ : a model of _Vibrio parahaemolyticus_ infection," *Fish & Shellfish Immunology*, vol. 56, pp. 388–396, 2016.

[33] X. Guo, C. Ji, X. Du, J. Ren, and Q. Zhang, "Comparison of gene expression responses of zebrafish larvae to _Vibrio parahaemolyticus_ infection by static immersion and caudal vein microinjection," *Aquaculture and Fisheries*, vol. 6, no. 3, pp. 267–276, 2021.

[34] X. Zhang, X. Tang, N. T. Tran et al., "Innate immune responses and metabolic alterations of mud crab (_Scylla paramamosain_) in response to _Vibrio parahaemolyticus_ infection," *Fish & Shellfish Immunology*, vol. 87, pp. 166–177, 2019.

[35] L. Zhang and K. Orth, "Virulence determinants for _Vibrio parahaemolyticus_ infection," *Current Opinion in Microbiology*, vol. 16, no. 1, pp. 70–77, 2013.

[36] Q. Cai and Y. Zhang, "Structure, function and regulation of the thermostable direct hemolysin (TDH) in pandemic _Vibrio parahaemolyticus_," *Microbial Pathogenesis*, vol. 123, pp. 242–245, 2018.

[37] P. Paria, H. J. Chakraborty, B. K. Behera, P. K. Das Mohapatra, and B. K. Das, "Computational characterization and molecular dynamics simulation of the thermostable direct hemolysin-related hemolysin (TRH) amplified from Vibrio parahaemolyticus," *Microbial Pathogenesis*, vol. 127, pp. 172–182, 2018.

[38] J. W. Costerton, L. Montanaro, and C. R. Arciola, "Biofilm in implant infections: its production and regulation," *International Journal of Artificial Organs*, vol. 28, no. 11, pp. 1062–1068, 2005.

[39] X. Song, Y. Ma, J. Fu, A. Zhao, and Y. Zhao, "Effect of temperature on pathogenic and non-pathogenic Vibrio parahaemolyticus biofilm formation," *Food Control*, vol. 73, pp. 485–491, 2016.

[40] Y. Yin, P. Ni, D. Liu et al., "Bacteriophage potential against _Vibrio parahaemolyticus_ biofilms," *Food Control*, vol. 98, pp. 156–163, 2019.

[41] F. Fei, B. Liu, X. Gao, X. Wang, Y. Liu, and H. Bin, "Effects of supplemental ultraviolet light on growth, oxidative stress responses, and apoptosis-related gene expression of the shrimp _Litopenaeus vannamei_," *Aquaculture*, vol. 520, p. 735013, 2020.

[42] Ç. U. Pala and A. K. Toklucu, "Effects of UV-C light processing on some quality characteristics of grape juices," *Food and Bioprocess Technology*, vol. 6, no. 3, pp. 719–725, 2013.

[43] B. G. Petri, R. J. Watts, A. L. Teel, S. G. Huling, and R. A. Brown, "Fundamentals of ISCO using hydrogen peroxide," in *In situ chemical oxidation for groundwater remediation*, pp. 33–88, Springer, 2011.

[44] A. P. Fraise, J. Y. Maillard, and S. Sattar, *Russell, Hugo & Ayliffe's Principles and Practice of Disinfection, Preservation & Sterilization*, 2013, Blackwell Pub.

[45] S. H. Chang, "Gold(III) recovery from aqueous solutions by raw and modified chitosan: a review," *Carbohydrate Polymers*, vol. 256, no. 5, p. 117423, 2020.

[46] N. A. Chudasama and A. K. Siddhanta, "Facile synthesis of nano-sized agarose based amino acid–its pH-dependent protein-like behavior and interactions with bovine serum albumin," *Carbohydrate Research*, vol. 417, pp. 57–65, 2015.

[47] S.-J. Ryu, H. Jung, J.-M. Oh, J.-K. Lee, and J.-H. Choy, "Layered double hydroxide as novel antibacterial drug delivery system," *Journal of Physics and Chemistry of Solids*, vol. 71, no. 4, pp. 685–688, 2010.

[48] F. Ahmed, S. M. Faisal, A. Ahmed, and Q. Husain, "Beta galactosidase mediated bio-enzymatically synthesized nano-gold with aggrandized cytotoxic potential against pathogenic bacteria and cancer cells," *Journal of Photochemistry and Photobiology B: Biology*, vol. 209, p. 111923, 2020.